Simulation Design of a Wells Turbine Overspeed Protection System for an OWC-Type Ocean Wave Power Plant Based on Speed Sensor and Soft Braking Control

Habib Alifian Achmad Firmansyah[1], Artono Raharjo[2], Lee Tsai Cheng[3]
Mechanical Engineering Study Program, Faculty of Engineering, Islamic University of Malang
e-mail: firmansyahachmad284@gmail.com

ABSTRACT

Oscillating Water Column (OWC) ocean wave power plants use a Wells turbine that is highly sensitive to fluctuating wave energy, making overspeed a critical operational risk. This study designs and simulates a speed-sensor-based overspeed protection system using inverter-driven soft braking control for a Wells turbine-generator system, modeled in MATLAB/Simulink. Six scenarios combining two initial overspeed conditions (1710 rpm and 1800 rpm) with three braking resistor values (90 Ω, 100 Ω, and 110 Ω) were simulated against a reference speed of 1440 rpm. Results show that the protection system activates immediately and reduces speed toward the reference in all scenarios, with response times of 7.5-10.5 s and a final error below 0.01%. The 1710 rpm scenario with a 90 Ω resistor produces the most balanced response (minimum speed 1415.96 rpm, response time 9.2 s, maximum braking torque 8.24 N.m), while for the 1800 rpm condition the 100 Ω resistor gives a more stable response. A larger braking resistor slows the response time, and a higher initial speed increases the required braking torque, angular deceleration, and braking power.

Keywords: Oscillating Water Column, Wells turbine, overspeed protection, soft braking, speed sensor, MATLAB/Simulink.

INTRODUCTION

Ocean Wave Power Plants (PLTGL) are a form of renewable energy utilization that has developed because they exploit naturally available and sustainable marine energy potential, and wave energy continues to be encouraged through research and demonstration projects worldwide [1]. Oscillating Water Column (OWC) technology utilizes the oscillation of the water surface inside a chamber due to sea waves; the up-and-down water movement compresses and decompresses the air inside the chamber, producing airflow through a turbine as part of the power take-off system [2].

The Wells turbine is a self-rectifying air turbine widely used in OWC systems because it produces one-directional rotation despite the periodically reversing airflow, simplifying integration with the generator. However, it is sensitive to changes in operating conditions, so speed control is required to maintain system stability [2]. Sea waves are difficult to predict, and momentary energy peaks can push the system beyond its rated speed, which is the main trigger of overspeed; protection must therefore be designed to address extreme scenarios, not only nominal operating conditions [3]. Overspeed control can be applied on the pneumatic side by dumping excess air energy before it reaches the turbine, or on the generator side using inverter-based power electronics that enable precise torque and current regulation for smoother and more adaptive speed control [4].

This research is entitled "Simulation Design of a Wells Turbine Overspeed Protection System for an OWC-Type Ocean Wave Power Plant Based on Speed Sensor and Soft Braking Control" and focuses on simulating the mechanical response of the turbine-generator system under overspeed conditions and designing a protection mechanism based on a speed sensor and inverter-based soft braking control. The simulation observes changes in rotational speed, braking torque, response time, overshoot, mechanical braking power, and their influence on system operating stability, with the aim of describing the mechanical response characteristics of the turbine-generator system and identifying the control parameters that most influence safe operation.

RESEARCH METHOD

The research method used is a quantitative method with a numerical simulation and system design approach. The overspeed protection system for a Wells turbine in an OWC-type ocean wave power plant is modeled using MATLAB/Simulink. Research data are obtained from simulation outputs, including rotational speed response, braking torque, response time, overshoot, angular deceleration, and mechanical braking power. The independent variables are the initial turbine speed under overspeed conditions and the braking resistor value used in the soft braking system; the dependent variables are the turbine speed after protection activation, the response time of the protection system, and the speed overshoot relative to the overspeed threshold. The turbine mechanical parameters, OWC configuration, safe-speed threshold, equivalent moment of inertia, sensor configuration, and simulation settings are held constant as control variables.

The simulation model consists of a turbine input torque block, a rotational dynamics block, a speed sensor block, an overspeed controller, a PI controller, and a soft braking block, as shown in Figure 1. The net torque, obtained from the difference between turbine input torque and braking torque, drives the rotational dynamics block that produces the system speed response over time. The speed signal is converted into rpm and Hz, and is used as input for the overspeed controller and the PI controller, which compares actual speed with the reference of 24 Hz (1440 rpm). When overspeed is detected, the protection signal becomes active and the PI controller generates a correction signal that drives the soft braking block to produce braking torque, which is fed back as opposing torque to reduce rotational speed.

The main simulation input is the initial turbine speed, namely 1710 rpm (28.5 Hz) and 1800 rpm (30 Hz), both above the overspeed threshold of 1500 rpm (25 Hz) and the reference speed of 1440 rpm (24 Hz). The braking resistor variations used are 90 Ω, 100 Ω, and 110 Ω. The complete simulation parameters are summarized in Table 1.

Table 1. Simulation Parameters

No.	Parameter	Value	Unit
1	Simulation time	60	s
2	Initial speed 1	1710	rpm
3	Initial speed 2	1800	rpm
4	Overspeed threshold	1500	rpm
5	Reference speed	1440	rpm
6	Average input torque (T_mean)	5	N.m
7	Braking constant (K_brake)	1000	N.m.Ω
8	Braking resistor variation	90, 100, 110	Ω

The combination of two initial-speed variations and three braking-resistor variations produces six simulation scenarios, as listed in Table 2. Each scenario is run for a simulation duration of 60 s, and results are compared based on speed response, protection activation, braking torque, response time, overshoot, angular deceleration, braking power, and system stability.

Table 2. Overspeed Simulation Scenarios

Scenario	Initial Speed	Braking Resistor
1	1710 rpm	90 Ω
2	1710 rpm	100 Ω
3	1710 rpm	110 Ω
4	1800 rpm	90 Ω
5	1800 rpm	100 Ω
6	1800 rpm	110 Ω

RESULTS AND DISCUSSION

The MATLAB/Simulink model of the overspeed protection system is shown in Figure 1. Based on the simulation, the overspeed controller (OC) signal is active (value 1) from the beginning of every scenario because all simulations start from an initial speed already above the 1500 rpm threshold; the protection system therefore begins generating a correction signal to the soft braking mechanism from t = 0 s.

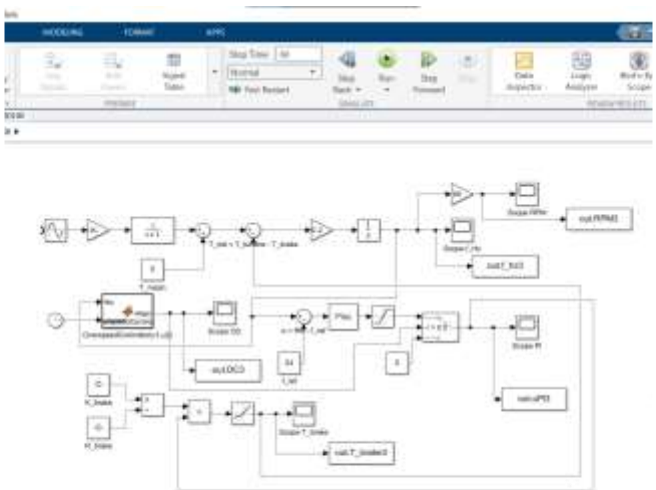

Figure 1. MATLAB/Simulink model of the overspeed protection system

In the 1710 rpm speed group, all three braking-resistor variations reduce the speed from the overspeed condition toward the 1440 rpm

reference. The 90 Ω resistor produces the smallest undershoot, with a minimum speed of 1415.96 rpm, while the 110 Ω resistor produces the largest undershoot, at 1361.69 rpm, indicating a stronger transient as the resistor value increases. In the 1800 rpm group, the 90 Ω resistor produces the deepest undershoot within this speed group, with a minimum speed of 1376.07 rpm, because it also generates the fastest and strongest braking action. All six scenarios ultimately converge to a final speed within 0.01% of the 1440 rpm reference.

The overshoot of the initial speed relative to the 1500 rpm threshold is OS = 210 rpm (14%) for the 1710 rpm condition and OS = 300 rpm (20%) for the 1800 rpm condition, calculated from Equation (1):

$$OS(\%) = ((N_{max} - N_{threshold}) / N_{threshold}) \times 100\% \quad (1)$$

Braking torque, angular deceleration, and mechanical braking power all increase with initial speed. In the 1710 rpm group the maximum braking torque ranges from 8.03-8.24 N.m, angular deceleration from 2.28-2.34 rad/s², and braking power from 1437.93-1475.54 W. In the 1800 rpm group these ranges rise to 9.09-10.14 N.m, 3.21-3.70 rad/s², and 1713.47-1911.39 W, respectively, because the higher initial speed carries greater mechanical energy that must be dissipated. Response time follows the opposite trend with respect to resistor value: increasing the braking resistor from 90 Ω to 110 Ω lengthens the response time from 9.2 s to 10.5 s in the 1710 rpm group, and from 7.5 s to 8.9 s in the 1800 rpm group, showing that a smaller braking resistor produces a faster response but a deeper undershoot. A full comparison of the six scenarios is given in Table 3, and the response-time comparison is shown in Figure 2.

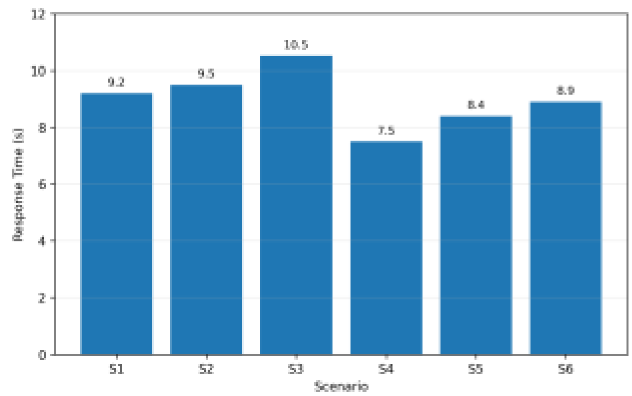

Figure 2. Comparison of response time between the six simulation scenarios

Scen.	Initial Speed	Resistor	Min. RPM	Response Time	T_brake Max	Angular Decel.	Braking Power
1	1710 rpm	90 Ω	1415.96	9.2 s	8.24 N.m	2.28 rad/s²	1475.54 W
2	1710 rpm	100 Ω	1402.41	9.5 s	8.05 N.m	2.28 rad/s²	1441.51 W
3	1710 rpm	110 Ω	1361.69	10.5 s	8.03 N.m	2.34 rad/s²	1437.93 W
4	1800 rpm	90 Ω	1376.07	7.5 s	10.14 N.m	3.70 rad/s²	1911.39 W
5	1800 rpm	100 Ω	1397.28	8.4 s	9.51 N.m	3.43 rad/s²	1792.64 W
6	1800 rpm	110 Ω	1389.27	8.9 s	9.09 N.m	3.21 rad/s²	1713.47 W

Table 3. Comparison of Results Between Simulation Scenarios

The simulation model was validated by checking internal consistency between blocks, manual recalculation of key outputs (e.g., the 1710 rpm/90 Ω braking power of 8.24 N.m x 179.07 rad/s = 1475.54 W), and trend consistency, in which the

1800 rpm group consistently shows larger overshoot, torque, deceleration, and braking power than the 1710 rpm group, as expected from rotational mechanics. The response trend was also compared against experimental literature. Torresi et al. tested a Wells turbine at 1750 rpm under unsteady flow [5], close to the 1710-1800 rpm range used here (2.29% and 2.86% difference, respectively), and reported transient torque changes consistent with the RPM reduction, undershoot, and torque variation observed in this simulation. Carrelhas et al. showed that the OWC turbine-generator system at the Mutriku plant requires a control strategy to keep the power take-off within safe limits [3], consistent with the present results in which the soft braking mechanism activates once speed exceeds the threshold and drives the system back toward the reference; the absolute torque magnitudes differ because of the difference in system scale, inertia, and turbine type.

Overall, the best response for the 1710 rpm overspeed condition is obtained with a 90 Ω braking resistor, which combines the smallest undershoot (1415.96 rpm), a response time of 9.2 s, a maximum braking torque of 8.24 N.m, an angular deceleration of 2.28 rad/s², a braking power of 1475.54 W, and a final error of 0.0007%. For the higher overspeed condition of 1800 rpm,

the 100 Ω resistor provides a more balanced response, since the 90 Ω resistor, although the fastest, produces a deeper undershoot and a stronger transient response within the 1800 rpm group. This indicates that the resistor value producing the largest torque or fastest response is not necessarily the best choice, since the overall response must also be judged by undershoot and final stability.

CONCLUSION

The simulated Wells turbine overspeed protection system, based on a speed sensor and inverter-driven soft braking control, is able to operate in all six scenarios. The protection system is active from the start of the simulation because all initial speeds exceed the 1500 rpm threshold, and it reduces speed toward the 1440 rpm reference with a final error below 0.01% in every case. The initial speed of 1710 rpm produces an overshoot of 210 rpm (14%), while 1800 rpm produces an overshoot of 300 rpm (20%); variations in initial speed and braking resistor affect response time, minimum RPM, braking torque, angular deceleration, braking power, and final stability. The best overall response is obtained at 1710 rpm with a 90 Ω braking resistor (minimum RPM 1415.96, response time 9.2 s, maximum torque 8.24 N.m, angular deceleration 2.28 rad/s², braking power 1475.54 W, final error 0.0007%), while for the higher 1800 rpm overspeed condition, a 100 Ω resistor gives a more balanced and stable response. Future work is recommended to validate these results experimentally, to expand the range of simulation parameters, to explore more adaptive control methods such as fuzzy or model predictive control, and to include the electrical aspects of the braking system.

NOMENCLATURE

J	equivalent moment of inertia of the turbine-generator system	[kg.m2]
N	rotational speed	[rpm]
f	rotational frequency	[Hz]
T_turbine	turbine input torque	[N.m]
T_brake	braking torque	[N.m]
P_brake	mechanical braking power	[W]
OS	speed overshoot	[rpm]
t_response	response time of the protection system	[s]

Greek letters

ω	angular speed of the turbine-generator system	[rad/s]
α	angular deceleration	[rad/s2]

REFERENCES

1. Magagna, D., & Uihlein, A., Wave and Tidal Current Energy - A Review of the Current State of Research Beyond Technology, Publications Office of the European Union, 2016.

2. Falcão, A. F. O., Wave Energy Utilization: A Review of the Technologies, Renewable and Sustainable Energy Reviews, Vol. 14, No. 3, pp. 899-918, 2010.

3. Carrelhas, A. A. D., Gato, L. M. C., & Henriques, J. C. C., Peak Shaving Control in OWC Wave Energy Converters: From Concept to Implementation in the Mutriku Wave Power

Plant, Renewable and Sustainable Energy Reviews, Vol. 180, 113299, 2023.

4. Darwish, A., & Aggidis, G. A., A Review on Power Electronic Topologies and Control for Wave Energy Converters, Energies, Vol. 15, No. 23, 9174, 2022.
5. Torresi, M., Pranzo, D., Pascazio, G., & Camporeale, S. M., Performance Characterization of a Wells Turbine under Unsteady Flow Conditions, AIP Conference Proceedings, Vol. 2191, 020149, 2019.
6. Gayathri, R., Wave Energy Conversion through Oscillating Water Columns, Journal of Marine Science and Engineering, Vol. 12, No. 2, 342, 2024.
7. Lekube, J., Garrido, I., Otaola, E., & Maseda, J., Flow Control in Wells Turbines for Maximizing Wave Energy Output, Sensors, Vol. 18, No. 2, 535, 2018.
8. Licheri, F., Review of Experimental Investigations on Wells Turbines, Energies, Vol. 18, No. 12, 3035, 2025.
9. Penalba, M., A Review of Wave-to-Wire Models for Wave Energy Converters, Energies, Vol. 9, No. 7, 506, 2016.
10. Rosati, M., Henriques, J. C. C., & Ringwood, J. V., Oscillating-Water-Column Wave Energy Converters: A Critical Review of Numerical Modelling and Control, Energy Conversion and Management: X, Vol. 16, 100322, 2022.
11. Uddin, M. N., Opoku, B., & Atkinson, D. J., Investigation of a Modified Wells Turbine for Wave Energy Conversion, Energies, Vol. 17, No. 15, 3638, 2024.
12. Impact of Turbine Operation Modes on Energy Conversion in OWC, Physics of Fluids, Vol. 37, No. 7, 075166, 2023.
13. Parrinello, S., Babarit, A., & Ferri, F., Adaptive and Energy-Maximizing Control of Wave Energy Converters: Review, arXiv, 2020.
14. Optimal Control and Layout Optimization of Wave Energy Converter Farms, arXiv, 2023.
15. M’zoughi, F., Garrido, I., Garrido, A. J., & De La Sen, M., Fuzzy Gain Scheduled-Sliding Mode Rotational Speed Control of an Oscillating Water Column, IEEE Access, 2020.
16. Rosati, M., Ringwood, J. V., & Henriques, J. C. C., Wave-to-Wire Efficiency Maximisation for Oscillating-Water-Column Systems, IFAC-PapersOnLine, 2023.
17. Szántó, A., Farkas, G., & Tóth, J., Simultaneous Measurement of the Moment of Inertia and Braking Torque of Electric Motors Applying Additional Inertia, Measurement, 2022.